We are IntechOpen, the world's leading publisher of Open Access books Built by scientists, for scientists

5,300
Open access books available

130,000
International authors and editors

155M
Downloads

Our authors are among the

154
Countries delivered to

TOP 1%
most cited scientists

12.2%
Contributors from top 500 universities

CLARIVATE ANALYTICS BOOK CITATION INDEX INDEXED

WEB OF SCIENCE™

Selection of our books indexed in the Book Citation Index in Web of Science™ Core Collection (BKCI)

Interested in publishing with us?
Contact book.department@intechopen.com

Numbers displayed above are based on latest data collected.
For more information visit www.intechopen.com

Chapter

A Note on Heat Transport with Aspect of Magnetic Dipole and Higher Order Chemical Process for Steady Micropolar Fluid

Assad Ayub, Hafiz A. Wahab, Zulqurnain Sabir and Adnène Arbi

Abstract

Heat transfer through non-uniform heat source/sink is the most significant aspect in view of many physical problems. Heat sink/source with heat transfer help to change the energy distribution in fluids, which consequently disturbs the particle deposition rate like as nuclear reactors, semiconductors and electronic devices. Further, also, the vital role of heat transfer is to enhance the thermal conductivity of micro sized solid particles in fluid. This study scrutinizes the heat transport of steady micropolar fluid via non-uniform heat sink/ source and mass transfer is scrutinized through higher order chemical reaction over a stretching surface with variable heat flux. Moreover, the velocity of micropolar fluid is studied by considering aspects of magnetic dipole and Newtonian heating; velocity slip conditions are also examined. The numerical results have been performed by using the well-known numerical shooting technique and comparison is performed with the Matlab built-in solver bvp4c. Geometrically explanation reveals the properties of numerous parameters that are the system parts. The observed outcomes show that the local skin-friction coefficient and Sherwood number values goes up with the increase of chemical reaction rate parameters and Schmidt numbers. Chemical reaction based parameters boosts up the rate of heat as well as mass transfer. The stress of wall couple increased by increasing the Schmidt and chemical parameters. Moreover, the plots of dimensionless parameters have been drawn, as well as some parameter results are tabulated.

Keywords: heat sink/source, heat transportation, magnetic dipole effect, Newtonian heating effect, micro polar fluid, slip velocity

1. Introduction

Magnetohydrodynamic (MHD) flow possesses real world applications for example, in the extrusion of a polymer sheet procedure, several product properties and significant control of cooling rate [1–3] and it controls under investigated physical state of the problem. Due to these important features of MHD flow, many researchers put their active attention towards the study of MHD and derived several numerical and theoretical results in mechanism of fluid flow. Andersson [4] did investigated about MHD flow of viscoelastic fluid with geometry of stretching

surface. Thermal radiation and MHD flow are interrelated and have massive applications in industries to know impact of thermal radiation on MHD flow explored by Raptis et al. [5]. Khan et al. [6] examined the MHD flow of boundary layer using the electric behavior of the fluid due to the cause of stretching in an elastic plane surface along the magnetic field. Abergel et al. [7] did work on different problems related to different physical situations and existence of such solutions to control problems, like boundary and boundary control in a channel. Moreover, he provided basic numerical algorithms named as conjugate gradient and steepest descent methods. Agrawal et.al [8] did research to investigate the transfer of heat with MHD flow by applying an unvarying suction over stretching surface. These investigations were classified to the Newtonian fluids. However, a novel phase to evaluate the theory of fluid using MHD flow is categorized by Aliakbar et al. [9]. Chemical reactive flow and its relationship with magnetic dipole impact on Cross model is investigated by khan et al. [10]. Mahanthesh et al. [11] explore preparation of numerical results related to MHD nanofluid flow with bidirectional linear stretching surface. Babu et al. [12] published his study about MHD slip flow of nanofluid with mass transfer via thermophoresis and Brownian motion. Nadeem et al. [13] examined time dependent MHD three- dimensional flow due to stretching/shrinking sheet.

Class of fluid that exhibits microscopic effects arising the phenomenon of micromotion of fluid particles is called micropolar fluid. This fluid consists of rigid macromolecule of individual motion that supports stress, body moment by spin inertia. These fluids contain micro-constituents that are capable of undergoing the rotation and have several practical applications in different areas, like depicting the attitude of exotic lubricants, turbulent shear flow, colloidal suspensions of nanofluid flow, human and animal blood, exotic lubricants, additive suspensions, colloidal fluids, liquid crystal, real fluids with interruptions and so forth [14]. Soundalgekar et al. [15] described an outstanding analysis of the micropolar fluids (MPFs) along with its applications. In another work, Soundalgekar et al. [16] explored the suction/injection effects in the flow passing over a semi-infinite porous plate using (MHD) MPF flow. Hady et al. [17] obtained the analytical results for the heat transfer model to a MPF using a non-stretching sheet. Ishak et al. [18] worked on the heat transfer over a stretching surface together with variable or uniform surface in (MHD) MPFs. Hassanien et al. [19] numerically discussed the suction/blowing effects on the heat/flow transfer using the MPF on a stretching surface. Hayat et al. [20] studied the two-dimensional mixed convection steady and stagnation point flow using (MHD) MPF on a stretching surface. Sajid et al. [21, 22] studied the true results for thin-film flows using MPF.

Vital role of thermal transport in various engineering problems, like as nuclear reactor cooling, metallurgical processes and continuous strips in which the performance of machine strongly dependent on the heat transfer rate and many hydrodynamic methods. Heat transfer through heat source/sink is most noteworthy aspect in view of many physical models. Heat generation/absorption can help to change the distribution energy in the fluid that consequently disturbs the particle deposition rate in the network like as semiconductors, nuclear reactors and electronic devices. Heat source/sink is assumed to be constant, temperature or space dependent. In this study, contains non-uniform heat sink/ source, i.e., temperature and space dependent heat source/sink. Motivated by the submissions of heat transfer with non-uniform heat source, numerous theoretical soundings have been discussed the heat transfer phenomenon in flows close to the stagnation point region [23]. Mabood et al. [24] used a shooting approach by considering the effects of thermal conductivity and variable viscosity using the MHD flow together with the transfer of heat in MPF through non uniform heat sink/source on a stretching sheet. The induction of flow is noticed because of an elastic sheet that is stretched

back as well as forward. Reddy et al. [25] explored the heat transport via heat generation and mass transfer effects on MHD flow together with inclined porous plate. Ravidran et al. [26] implemented the non-uniform single/double effects of slot suction/injection into an unstable mixed convection of an electrically conducting. Ghadikolaei et al. [27] expressed detailed study with MHD flow heat transport inspired by the thermal radiations as well as heat generation over a porous stretching sheet. Sandeep et al. [28] scrutinized the non-uniform heat source/sink influences, chemical reaction and mass transfer on the mixed convection flow using a MPF along with viscous dissipation.

Most significance aspect of daily life is chemical reaction, and without chemical reaction there is no concept of daily life because chemical reactions appear in biomedical field, agriculture, photosynthesis, reproduction system, chemical industry, even earth is fertile with the chemical reactions and used in many engineering applications. Chemical reaction helps to transport the mass of fluid flow and many researchers did work on transport of mass with taking different models of fluid like Cross, Carreau, sisko and Maxwell model of non-Newtonian fluid. Numerical interpretation related mass transfer of 3D Cross fluid with chemical reaction is made by [29]. First order chemical reaction impact in MPF is studied by damesh et al. [30]. Das et al. [31] published their investigations on chemical reaction and thermal radiation on heat and mass transfer flow of MHD micropolar fluid with rotating frame of reference Further Magyari et al. [32] depicted that Combined effect of heat generation or absorption and first-order chemical reaction on micropolar fluid flows over a uniformly stretched permeable surface. Effects of higher order chemical reaction on micropolar fluid and Influence of thermophoresis and chemical reaction on MHD micropolar fluid flow is discussed by [33]. Sajid et al. investigate the effects of variable molecular diffusivity, nonlinear thermal radiation, convective boundary conditions, momentum slip, and variable molecular diffusivity on Prandtl fluid past a stretching sheet [34].

From many year scientists did a lot of work with different fluid models to investigate heat/ mass transport through heat generation/ absorption and activation energy respectively. But here in this manuscript we deal transport of heat of MPF via non uniform heat sink/ source because this transportation deal disposition rate of particle (space dependent) and mass transfer is carried out through chemical reaction. Further linear velocity of MPF is scrutinized by magnetic dipole aspect and also angular movement of said fluid is made in this struggle.

The remaining parts of the paper are organized as: Section 2 shows the problem formulation, Section 3is designed the methodology, Section 4 shows the results and discussion, while conclusion is drawn in the final Section.

2. Problem formulation

The problem is formulated by using the equations based on conservation of mass, momentum, angular momentum, energy equation and concentration equations, written as:

$$\nabla.V = 0, \tag{1}$$

$$\rho[\nabla.V]V = -\nabla.p + (\mu + \chi)\nabla^2 V + k\nabla \times \Omega + \rho f, \tag{2}$$

$$\rho j[\nabla.V]\Omega = (\alpha_0 + \beta_0 + \gamma_0)\nabla[\nabla\Omega] - \gamma_0\nabla \times [\nabla \times \Omega] + \chi\nabla \times V - 2k\Omega + \rho l, \tag{3}$$

$$\rho c_p[V.\nabla]T = k\nabla^2 T - \varphi + Q \tag{4}$$

$$[\nabla.j] = D\nabla^2 C. \tag{5}$$

Consider a mixed convective steady state incompressible MPF passing over a porous plate that shrinks and stretches towards the velocity $u = su_w(x)$, whereas, $u_w(x) = ax$, a is a dimensional constant towards the flow axis (**Figure 1**). The sheet is stretched with the speed that vary with distance ℓ, further consider the flow region is $y > 0$ and B_0 is the magnetic field towards the$y$-axis. Presence of boundary layer heat transport, non-uniform source of heat, viscous dissipation along with magnetic field is presented. The components of micro-rotation and velocity components are $(0, 0, w)$ and $(u, v, 0)$, respectively. The basic equations are accounted in the presence of heat source and viscous dissipation. The flow positions are x and $y-$ axis along with the slip flow model, i.e., u-slip as well as the Newtonian heating are conditions as:

$$\frac{\partial u}{\partial x} + \frac{\partial v}{\partial y} = 0, \tag{6}$$

$$u\frac{\partial u}{\partial x} + v\frac{\partial u}{\partial y} = \left(\frac{\mu + \chi}{\rho}\right)\frac{\partial^2 u}{\partial y^2} + \frac{\chi}{\rho}\frac{\partial w}{\partial y} - \frac{\sigma\beta_0^2}{\rho}u + g_1\beta_C(C - C_\infty) + g_1\beta_T(T - T_\infty), \tag{7}$$

$$u\frac{\partial w}{\partial x} + v\frac{\partial w}{\partial y} = \left(\frac{\gamma}{\rho_j}\right)\frac{\partial^2 w}{\partial y^2} + \frac{\chi}{\rho_j}\left(2w + \frac{\partial w}{\partial y}\right), \tag{8}$$

$$u\frac{\partial T}{\partial x} + v\frac{\partial T}{\partial y} = \frac{k}{\rho C_p}\frac{\partial^2 T}{\partial y^2} + \frac{\mu}{\rho C_p}\left(\frac{\partial T}{\partial y}\right)^2 + \frac{q'''}{\rho C_p}, \tag{9}$$

$$u\frac{\partial C}{\partial x} + v\frac{\partial C}{\partial y} = D_m\frac{\partial^2 C}{\partial y^2} + D_m\frac{K_T}{T_m}\frac{\partial^2 T}{\partial y^2} - \xi(C - C_\infty). \tag{10}$$

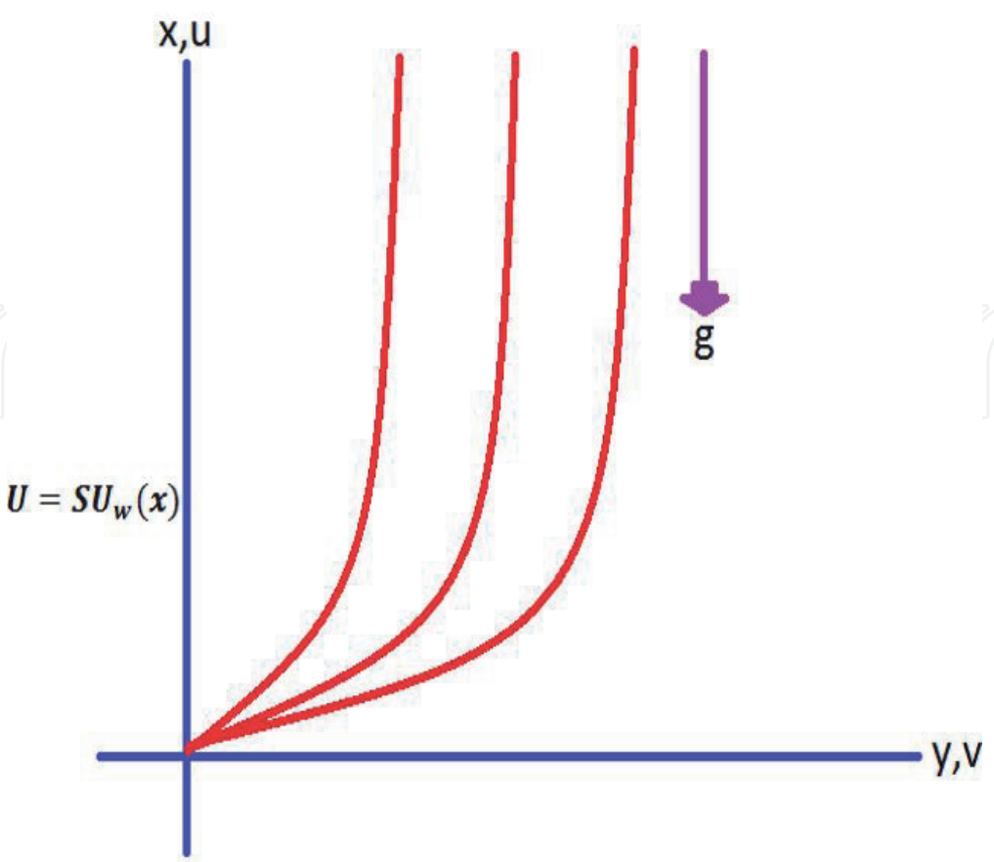

Figure 1.
Geometry of the problem.

To consider the spin gradient viscosity as

$$\gamma = \left(\mu + \frac{\chi}{2}\right) j = \mu\left(1 + \frac{K}{2}\right) j,\ K = \frac{\chi}{\mu} \text{ and } j = \frac{\nu}{a} \tag{11}$$

are the material parameter as well as micro inertia density, and $\nu = \frac{\mu}{\rho}$. Here q''' is the non-uniform heat source and defined as

$$q''' = (kU_w(x)/xv)\left[A^*(T_\infty)f'(\eta) + B^*(T - T_\infty)\right] \tag{12}$$

Moreover, $v_0 > 0$ and $v_0 < 0$ indicate the velocities based on suction as well as injection of the permeable plate.

The associated conditions are:

$$u = su_w(x) + u_{slip}, v = v_0, w = -n\frac{\partial u}{\partial y}, k\frac{\partial T}{\partial y} = -h_s T, C = C_w, \text{at } y = 0, \tag{13}$$

$$u \to 0, w \to 0, C \to C_\infty, T \to T_\infty, \text{ as } y \to \infty. \tag{14}$$

where n is constant and can be $0 \le n \le 1$, when, n = 0 leads to the concentration based micro-elements in MPF close to sheet that are do not rotate for $w = 0$, while n = 1 implies the turbulent flow. Moreover, u_{slip} represents the slip velocity and given as:

$$u_{slip} = \frac{2}{3}\left[\frac{3 - \varepsilon l^3}{\varepsilon} - \frac{3}{2}\frac{l - l^2}{k_n}\right] d\frac{\partial u}{\partial y} - \frac{1}{4}\left[l^4 + \frac{2}{k_n^2}\left(1 - l^2\right)\right] d^2\frac{\partial^2 u}{\partial y^2}, \tag{15}$$

$$u_{slip} = A\frac{\partial u}{\partial y} + B\frac{\partial^2 u}{\partial y^2}, \tag{16}$$

where l is $\min\left[\left(\frac{1}{k_n}\right), 1\right]$ that goes to $0 < l \le 1$. The Knudsen number is k_n and ε represents the coefficient of momentum that lies in the range of $0 < \varepsilon \le 1$. The term d remains positive and shows the mean molecular free path, while B is accordingly negative. By presenting the following suitable transformations as:

$$\Psi(x,y) = \sqrt{a\nu}xf(\eta), \phi(\eta) = \frac{C - C_\infty}{C_w - C_\infty}, \theta(\eta) = \frac{T - T_\infty}{T_\infty}, \eta = y\sqrt{\frac{a}{\nu}}, \tag{17}$$

$$w = axh(\eta)\sqrt{\frac{a}{\nu}}, u = \frac{\partial \Psi}{\partial y} = axf'(\eta), v = -\frac{\partial \Psi}{\partial x} = -\sqrt{a\nu}f(\eta), \tag{18}$$

where Ψ is called stream function. The momentum and heat equations are transformed to the governing momentum and heat transfer equations into the coupled ordinary differential equations as:

$$(1 + K)f''' + ff'' - f'^2 + Kh' - Mf' + \lambda\theta + \lambda A\phi = 0, \tag{19}$$

$$\left(1 + \frac{K}{2}\right)h'' + fh' - f'h - K\left(f'' + 2h\right) = 0, \tag{20}$$

$$\theta'' + \mathrm{Pr}f\theta' + Ec\left(f''\right)^2 + A^*f' + B^*\theta = 0, \tag{21}$$

$$\phi'' + Sc[f\theta' + Sr\theta'' + C_m\phi'] = 0, \tag{22}$$

The boundary conditions are

$$\begin{cases} f = f_w, f' = s + \alpha f'' + \beta f''', h = -nf'', \theta' = -\delta(1+\theta), \phi = 1 \text{ at } \eta = 0, \\ f'(\eta) \to 0, h(\eta) \to 0, \theta(\eta) \to 0, \phi(\eta) \to 0, \text{as } \eta = \infty. \end{cases} \tag{23}$$

Where the dimensionless parameters are defined as:
$K = \frac{\chi}{\mu}$, $\Pr = \frac{\mu C_p}{k}$, $Ec = \frac{a^2 x^2}{c_p}$, $M = \frac{\sigma B_0^2}{\rho a}$, $\lambda = \frac{Gr_x}{Re_x}$, $Gr_x = \frac{g\beta_T T_\infty x}{a\nu}$, $C_m = \frac{\xi}{a}$, $\beta = \frac{h_s}{k}\sqrt{\frac{\upsilon}{a}}$, $Sr = \frac{D_m k_T (T_w - T_\infty)}{T_m \nu (C_w - C_\infty)}$, $Du = \frac{D_m k_T \rho c_p (C_w - C_\infty)}{c_s c_p k (T_\infty)}$, $f_w = -[a\upsilon]^{-\frac{1}{2}} \nu_0$, $\mathrm{Re}_x = \frac{ax^2}{\upsilon}$, $\Lambda = \frac{g\beta_c (C_w - C_\infty)}{\beta_T T_\infty}$, $a = A\left(\frac{a}{\upsilon}\right) > 0$ and $\beta = \left(\frac{Ba}{\upsilon}\right) < 0$.

The physical quantities based on skin-friction coefficient c_f is $c_{fx} = -\frac{\tau_w}{\rho U_w^2}$ the wall shear stress, τ_w is given as:

$$\tau_{wx} = \left| (\mu + \chi)\frac{\partial u}{\partial y} + \chi w \right|_{y=0}, \tag{24}$$

The value of c_f is given as:

$$c_{fx}\,\mathrm{Re}_x{}^{1/2} = -(1 + K - nK) f''(\eta)\big|_{y=0}, \tag{25}$$

Here R_{ex} is the Reynolds number. The skin-friction coefficient defined in Eq. (18) does not contain the micro rotation term. In the temperature field, the heat transfer rate is defined as:

$$Nu_x = -\frac{x q_w}{T - T_\infty}, \text{where } q_w = \left(\frac{\partial T}{\partial T}\right)_{y=0}. \tag{26}$$

The local Nusselt number is shown as:

$$Nu_x (\mathrm{Re}_x)^{-0.5} = \delta\left(1 + \frac{1}{\theta(\eta)}\right)_{\eta=0}. \tag{27}$$

The couple stress is given as:

$$M_x = \frac{-m_w}{\rho x (ax)^2}, m_w = \left(\mu + \frac{\chi}{2}\right) j \left[\frac{\partial w}{\partial y}\right]_{y=0}, M_x \,\mathrm{Re}_x = -\left(1 + \frac{K}{2}\right) h'(0). \tag{28}$$

Furthermore, the mass diffusion flux and Sherwood number become as:

$$Sh_x = \frac{x S_m}{(C - C_w)}, \tag{29}$$

$$S_m = \left(\frac{\partial C}{\partial y}\right)_{y=0}. \tag{30}$$

Finally, Sherwood number becomes as:

$$Sh_x / (\mathrm{R_{ex}})^{-1/2} = (-\phi(\eta))_{\eta=0}. \tag{31}$$

The results of the above nonlinear equations have been performed by using a well-known shooting technique and comparison is performed with the bvp4c. The

shooting technique is fast convergent scheme and have been used to solve the extensive applications of fluid dynamics [35–40]. For the implementations of the shooting scheme, the boundary value system has been converted into the initial value equations. The nonlinear Eqs. (19)-(22) take the form as:

$$\begin{cases} f = n_1,\ f' = n_2,\ f'' = n_3, \\ n_3' = \dfrac{1}{1+K}\left[Mn_2 - n_1n_3 + n_2^2 - Kn_5 - \lambda n_6 - \lambda\Lambda n_8\right], \\ n_4 = h,\ n_4' = n_5, \\ n_5' = \dfrac{1}{\left(1+\dfrac{K}{2}\right)}\left[n_2n_4 - n_1n_5 + K(2n_4 + n_3)\right], \\ n_6 = \theta, \theta' = n_7, \\ n_7' = \left[-\mathrm{Pr}n_1n_7 - Ecn_3^2 - (A^*n_2 + B^*n_6)\right], \\ n_8 = \phi, \phi' = n_9, \\ n_9' = \left[-Sc\left(n_1n_7 + Srn_7' + C_mn_8\right)\right]. \end{cases} \tag{32}$$

The concerned initial conditions are written as:

$$\begin{cases} n_1 = f_w, n_2 = s + \alpha n_3 + \beta n_3', n_4 = -nn_3, n_7 = -\delta(1+n_6), n_8 = 1 \text{ at } \eta = 0, \\ n_2 = n_4 = n_6 = n_8 = 0 \text{ as } \eta = \infty. \end{cases} \tag{33}$$

Matlab bvp4c technique procedure is given as

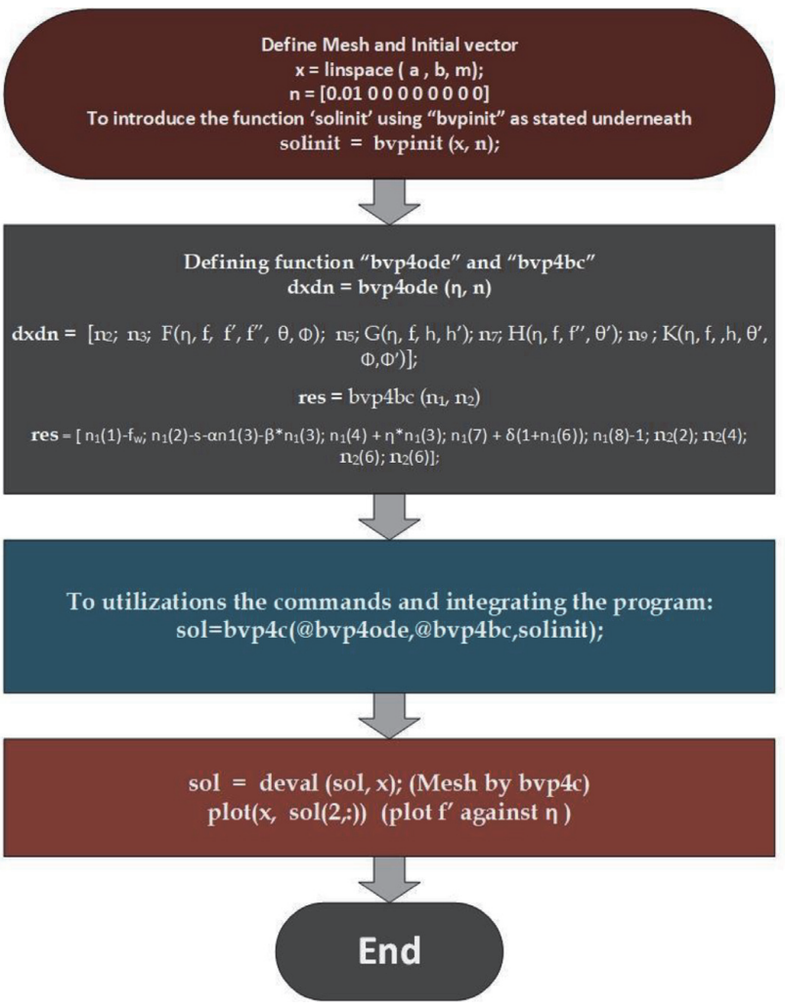

f_w	α	β	$-f''(0)$	$-f''(0)$	$-f''(0)$	$-f''(0)$
			Ref [27]	**Ref [28]**	**Bvp4c**	**Shooting**
2.0	0.5	−1	0.341213	0.3412	0.341214	0.341214
2.0	0.5	−2	0.203824	0.2038	0.203825	0.203825
2.0	1.0	−1	0.290548	0.2905	0.29057	0.29057
2.0	1.0	−2	0.184657	0.1846	0.18463	0.18463
3.0	0.5	−1	0.262681	0.2626	0.26281	0.26281
3.0	0.5	−2	0.147012	0.1470	0.14712	0.14712
3.0	1.0	−1	0.232017	0.2320	0.2314	0.2314
3.0	1.0	−2	0.136905	0.1369	0.13605	0.13605

Table 1.
Comparison value of $f''(\circ)$ for different values of the f_w.

For the satisfaction of the results, **Table 1** is provided is based on the literature results as well as the shooting and bvp4c for $f''(0)$ using numerous value of α by putting $K = 0$ and $M = 0$. The matching of the shooting and bvp4c results with the literature results [38, 39] depicts the satisfaction and validity of the scheme.

3. Results and discussions

In this section, the detail of the numerical results is presented to solve the system of nonlinear equations using shooting scheme. The effects of velocity profile, with physical parameters K, M, A, are examined, while Pr, Ec, A^*, B^*, are checked on temperature profile. Moreover, the influences of Sc, Sr, C_m is drawn on concentration profile through **Figures 2–14** as well as evaluation of physical quantities like c_f, Nu, M_x, Sh_x are provided.

3.1 Physical interpretation of parameters with velocity

The effects of parameter K, M, A, are examined by on the velocity profile and presented by **Figures 2–6**. Each parameter has its own impact for all the profiles along with its physical significance. As s is increasing, the sheet stretches due to this velocity increases $n \in (0, 1)$. When $n = 0$, then the MPF flow get closer to the sheet that are inept to rotate, likewise for $n = 1$ indicates the turbulent flow. The values of material constant 'K' enhance the velocity due to its materialistic properties. The velocity state decreases due to the Lorentz force by increasing the values of 'M'. Influence of the suction/injection parameter 'f_w' on the velocity component of the sheet shows an increment in the suction factor shows a decrease in the velocity together with the increment of the similarity values of the variable.

3.2 Physical interpretation of parameters with energy

The effects of different parameters are drawn on temperature profile are noticed in **Figures 7–12**. Temperature is decreasing for growing value of Pr, and B^* because of Pr reduces thermal conductivity and B^* is internal heat generation so negative values reduces the temperature. For also positive value of A^* temperature grows up. The energy intemperance exhibits a considerable increase with the wall temperature. This is reliable with the physical state because of elastic deformation

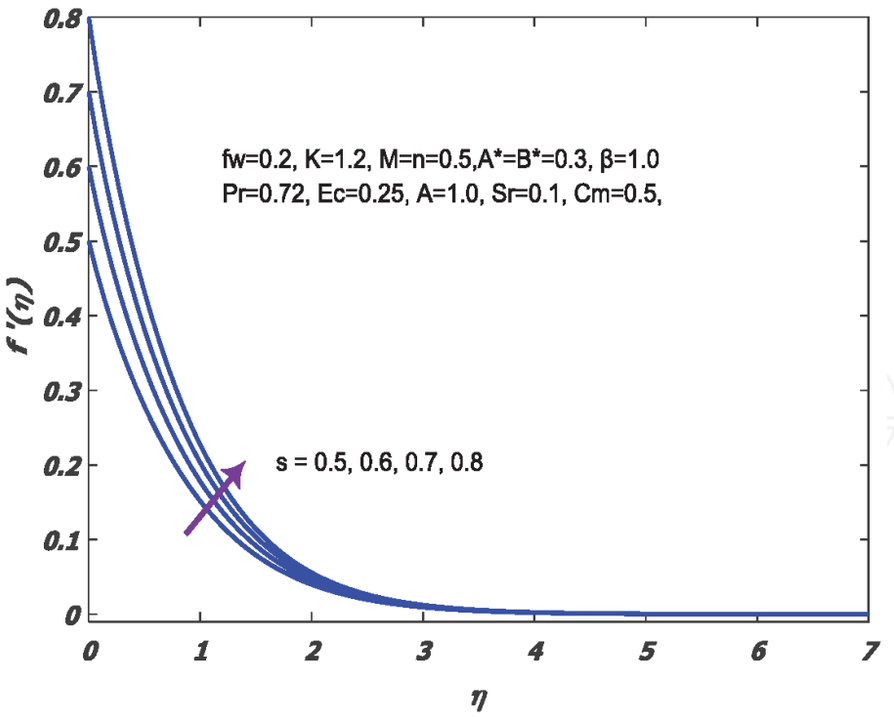

Figure 2.
s effects on f profile.

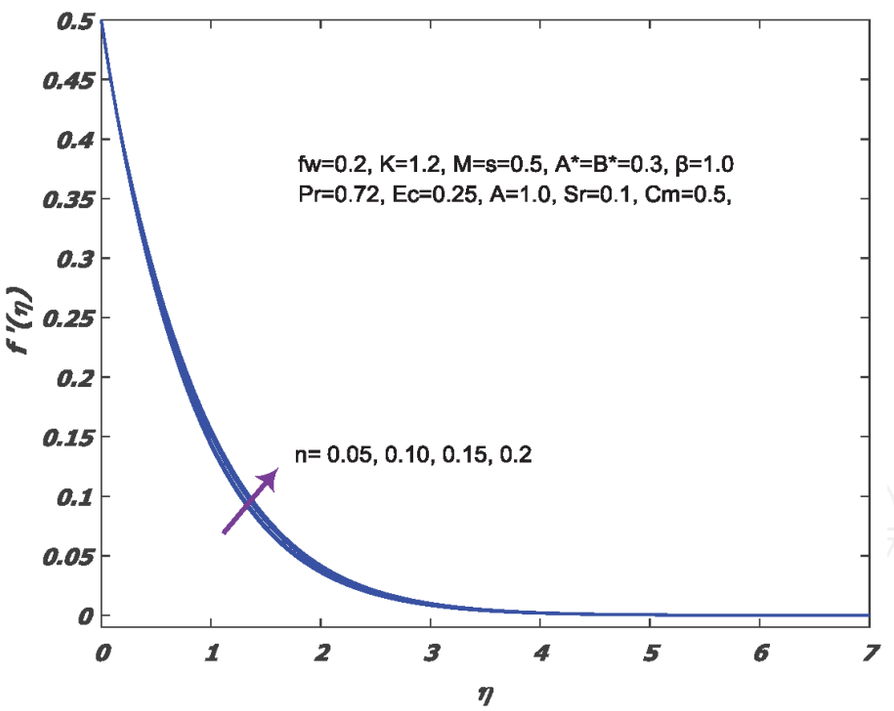

Figure 3.
n effects on f profile.

work, ohmic and frictional heating are considered that become the cause of incrementing the thermal based boundary layer.

3.3 Physical interpretation of parameters with concentration

Figures 11–14 depicts the angular velocity of MPF with attached parameters, for increasing value of Pr, n, M angular velocity increases. For growing Pr temperature

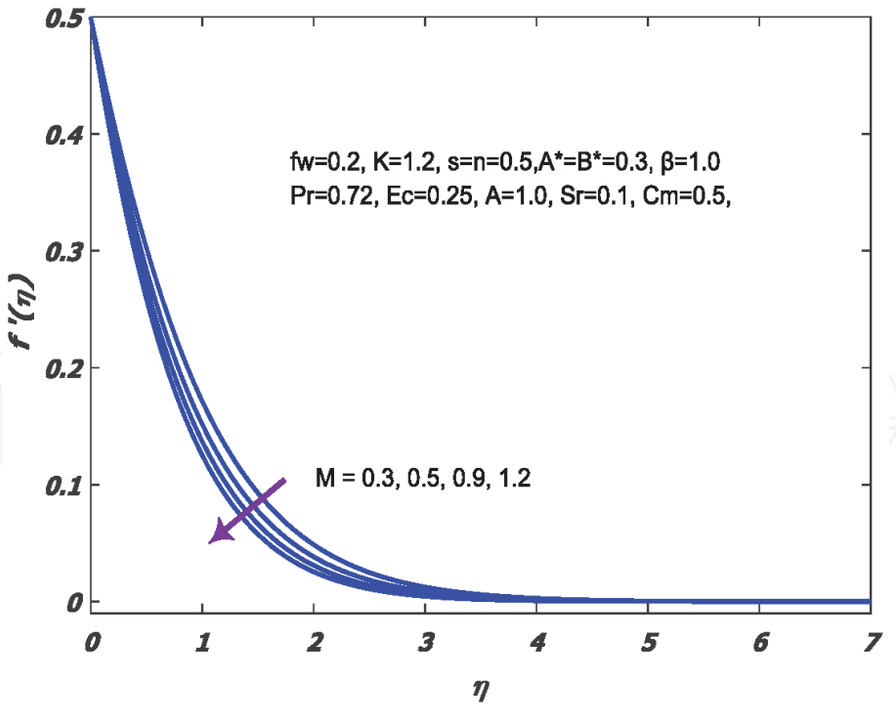

Figure 4.
M effects on f profile.

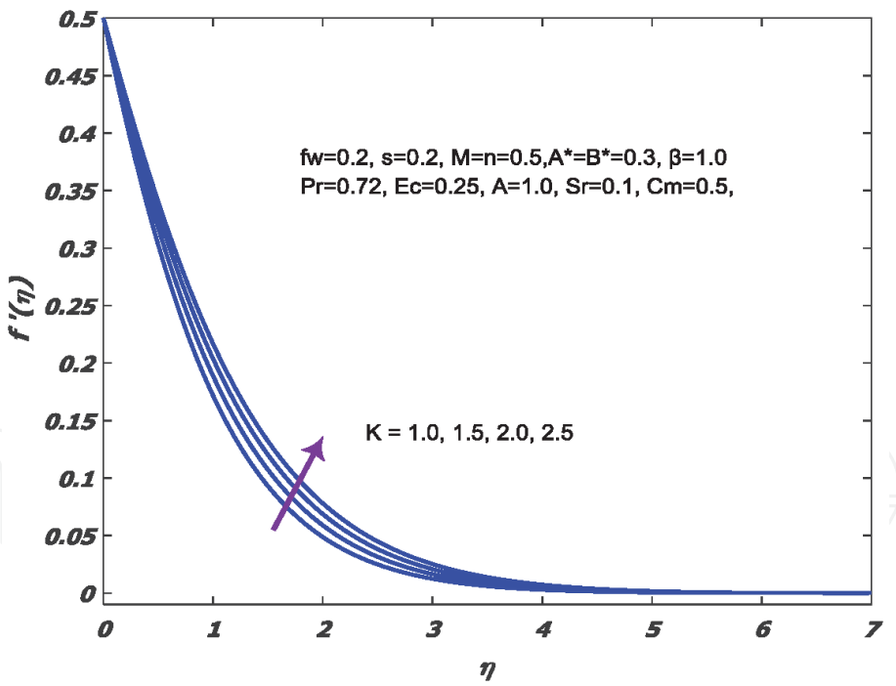

Figure 5.
K effects on f profile.

loses due to this movement of particle slows down due to this rotation gets down, and n is constant and there is no rotation when $n = 0$, so increase in n results growth in angular velocity. Similarly, a greater value of M produces Lorentz force due to this linear velocity downs but angular velocity uplifts. As the material parameter increases, it is observed that the boundary layer thickness increases due to this fact angular velocity decreases. The concentration profile became down with increment

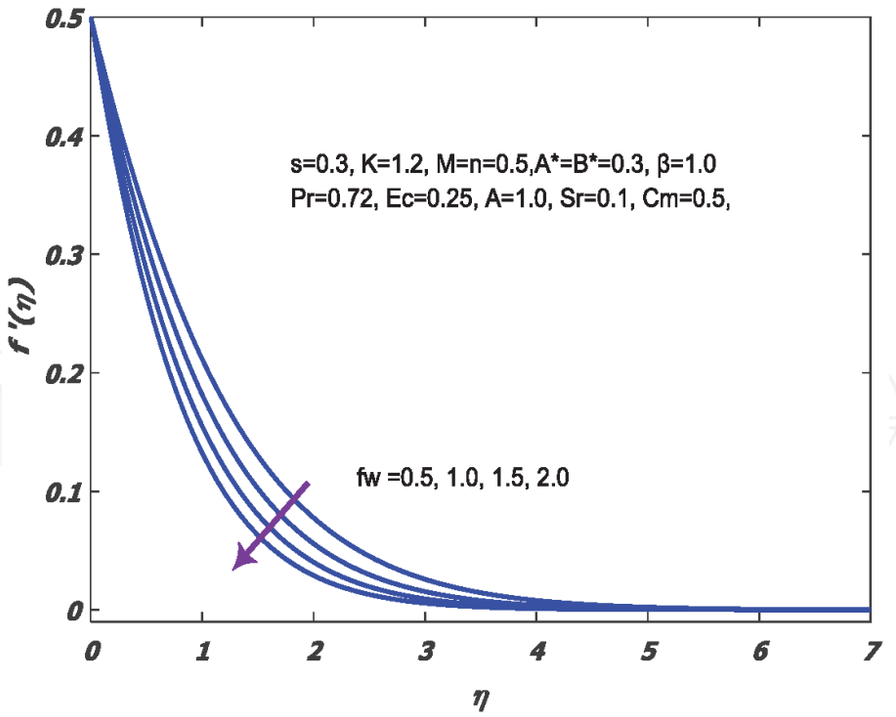

Figure 6.
f_w effects on f profile.

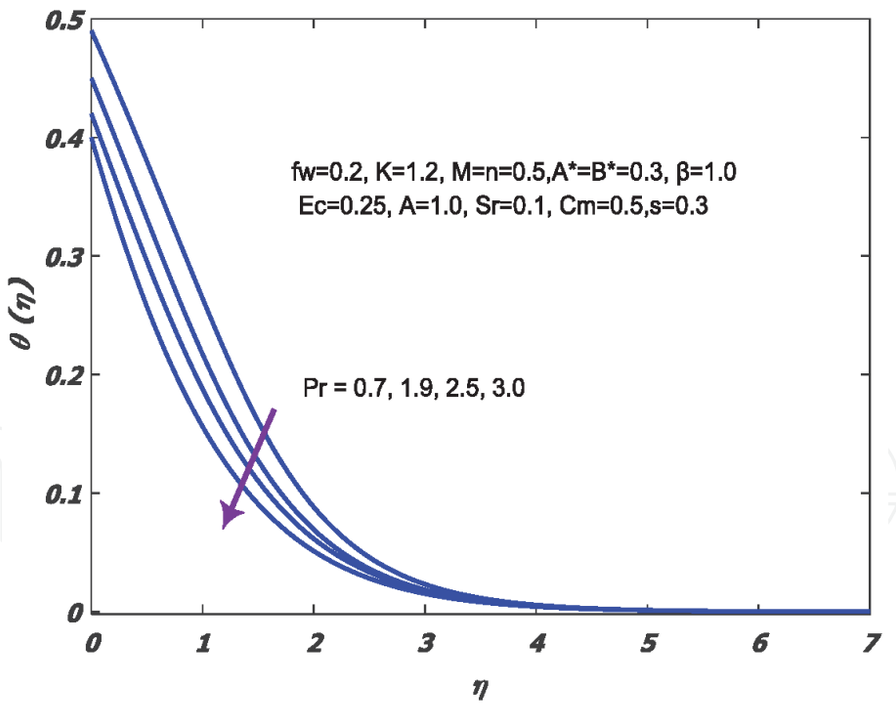

Figure 7.
Pr effects on θ profile.

of Pr, *Sc*, *Sr*, f_w and C_m. The increasing values of 'Pr' depicts that temperature decreases, as a result decrement is noticed in concentration. The concentration along with thickness of boundary layer decreases by enhancing the '*Sc*'. The Soret term, i.e., 'Sr' shows the temperature gradients effects on the profile of concentration. it is noticed that increment in 'Sr', temperature together with concentration increases (**Figures 15–19**).

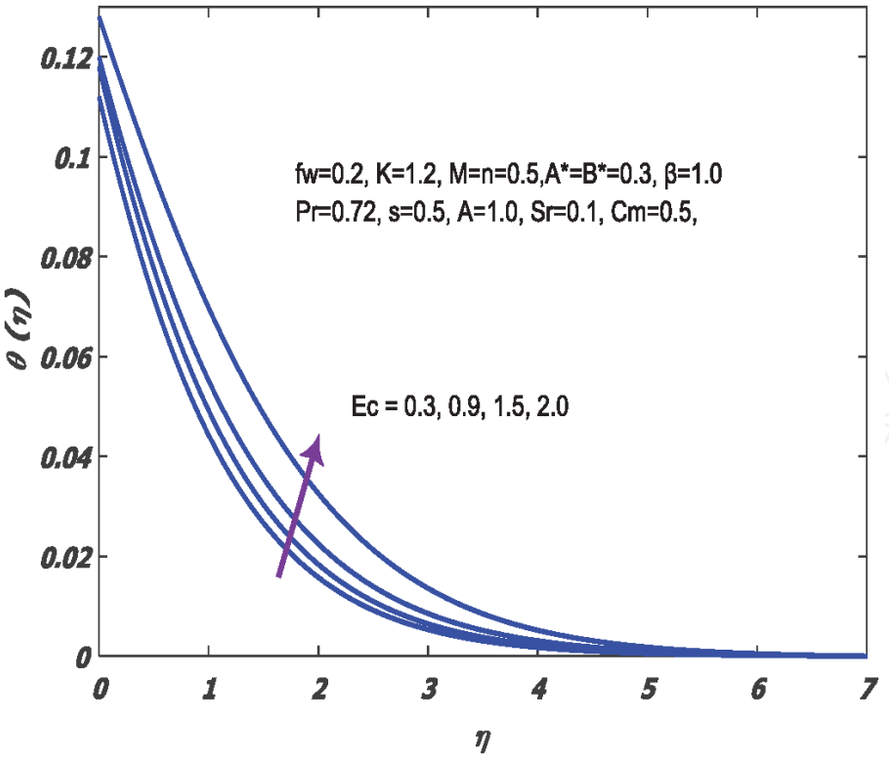

Figure 8.
E_c effects on θ profile.

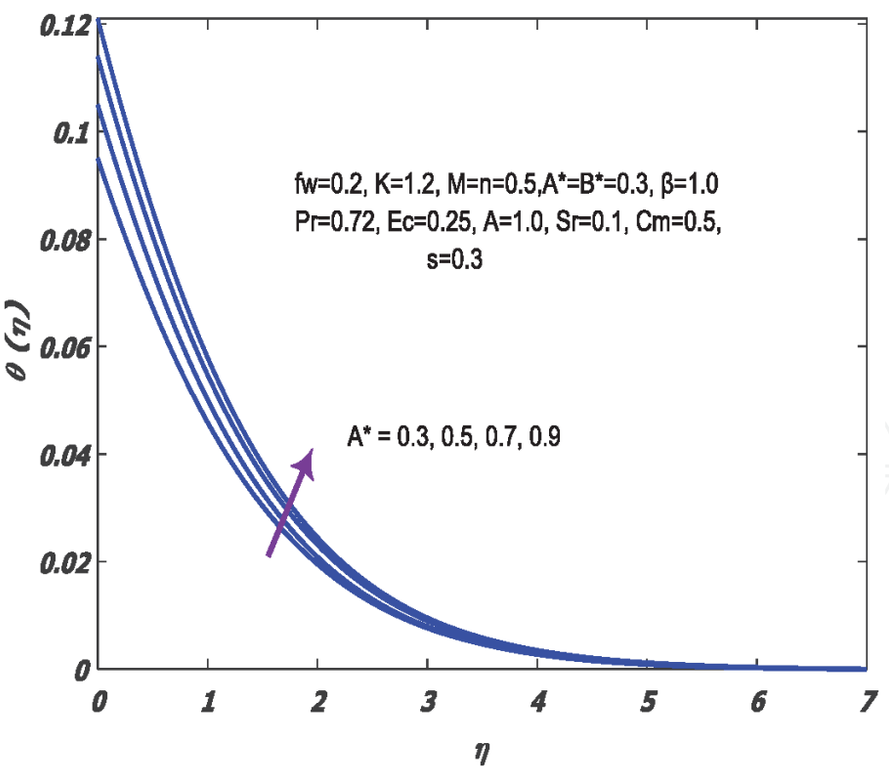

Figure 9.
A^* effects on θ profile.

3.4 Physical quantities interpretation

Skin friction is called the rate of heat transfer that shows the increment for greater value of K, Sc, C_m and decreases for growing values of A and f_w. Couple

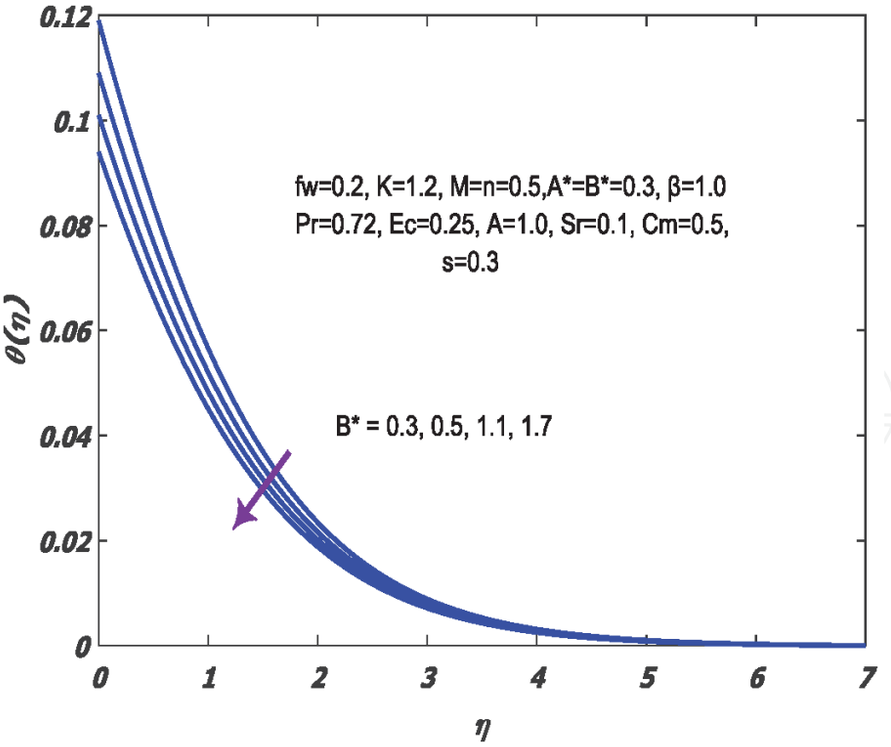

Figure 10.
B^* effects on θ profile.

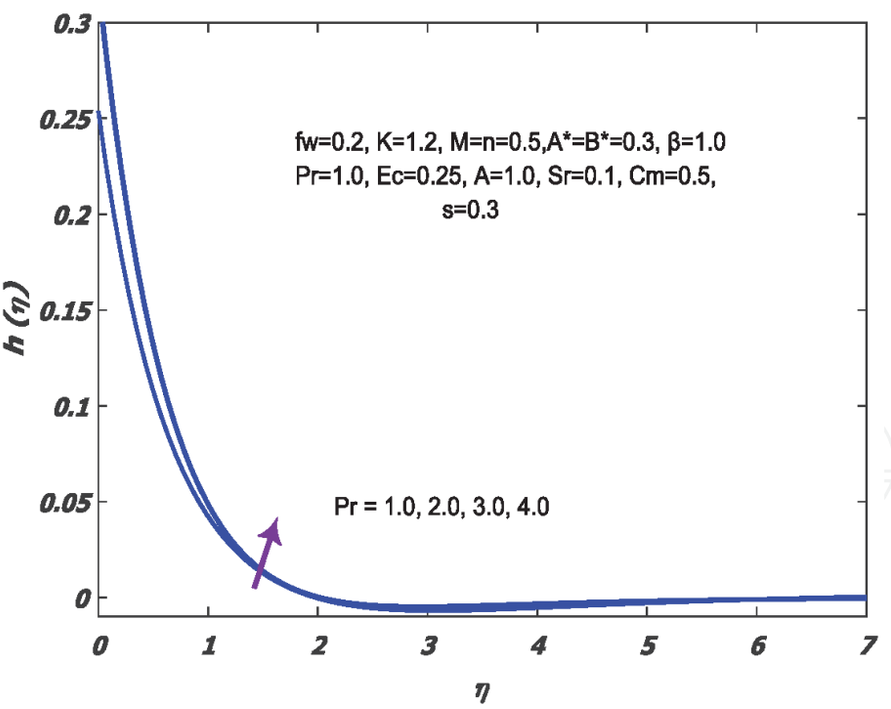

Figure 11.
Pr effects on h profile.

stress $M_x \operatorname{Re}_x$ values vary with parameter K. In this study, an increment is found in the couple stress $M_x \operatorname{Re}_x$ for growing value of K. Local mass diffusion flux namely Sh_x goes down for rising value of K and numerical result of the present study in **Table 2** is listed.

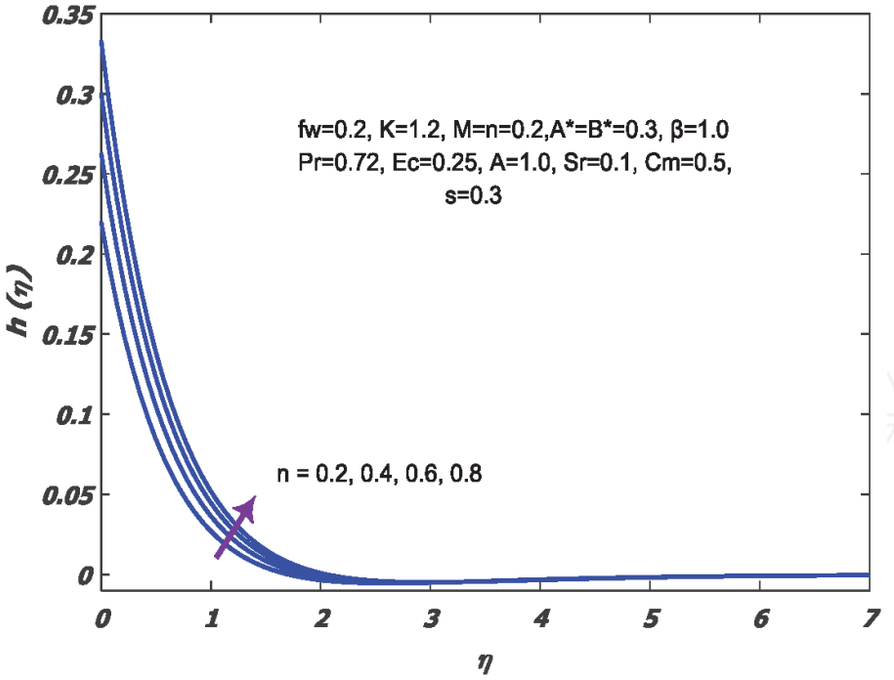

Figure 12.
n effects on h profile.

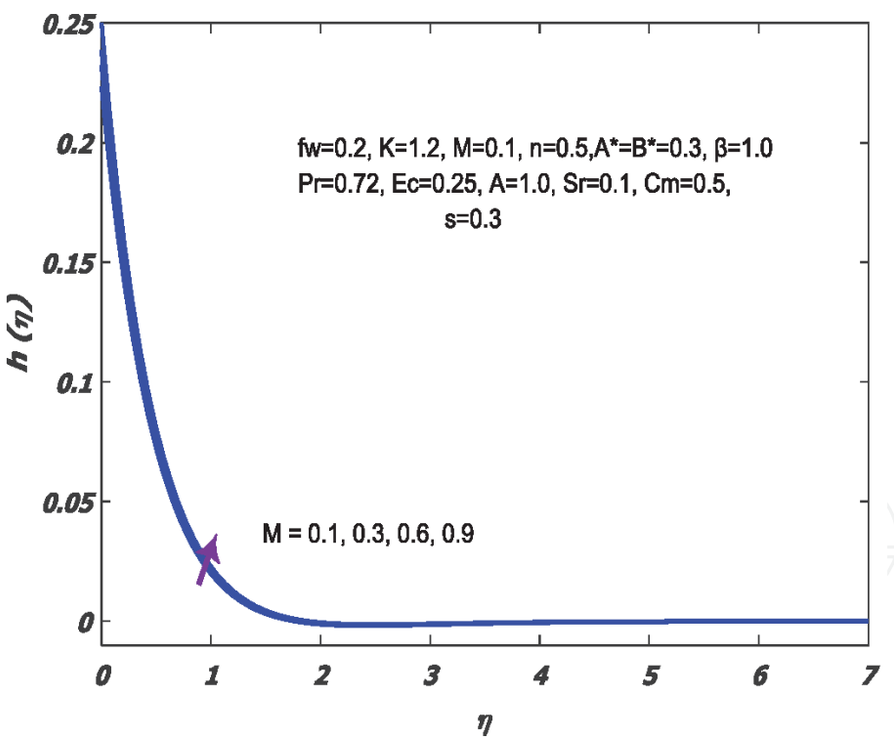

Figure 13.
M effects on h profile.

4. Concluding remarks

The key purpose of the current work is to discuss the effects of heat transportation and source/sink of heat with magnetic effect on boundary layer MPF. This study elaborates that angular velocity and linear velocity of MPF with different facts which impact on temperature and concentration of said fluid. For the

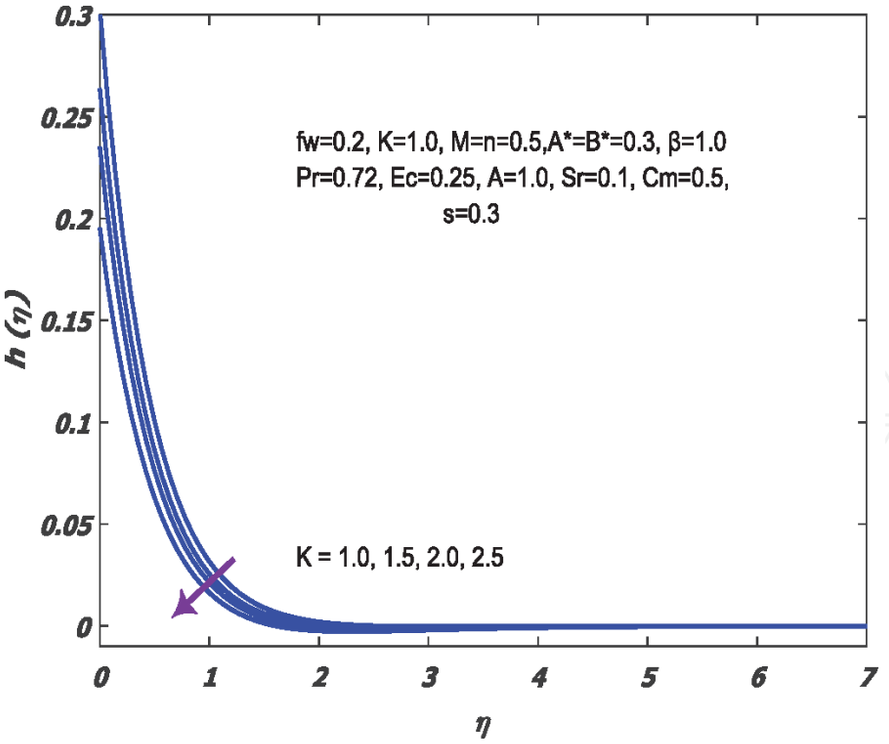

Figure 14.
K effects on h profile.

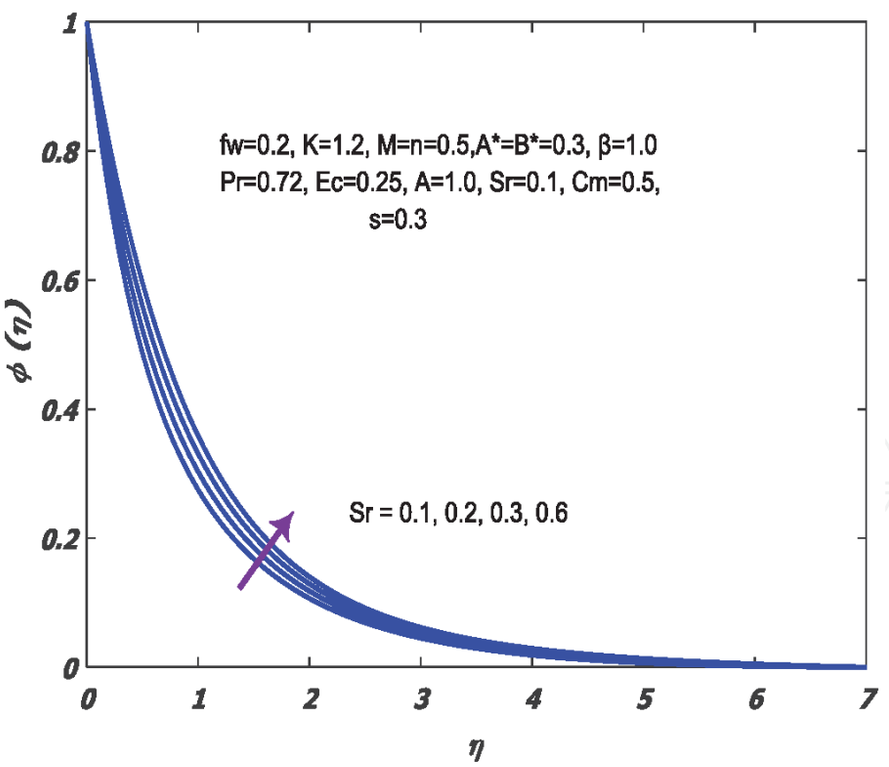

Figure 15.
S_r effects on ϕ profile.

numerical purpose, the shooting scheme has been implemented and comparison of the results with bvp4c is presented. Moreover, main key points of study are provided as:

1. Velocity of flow raises for growing of s, n, K.

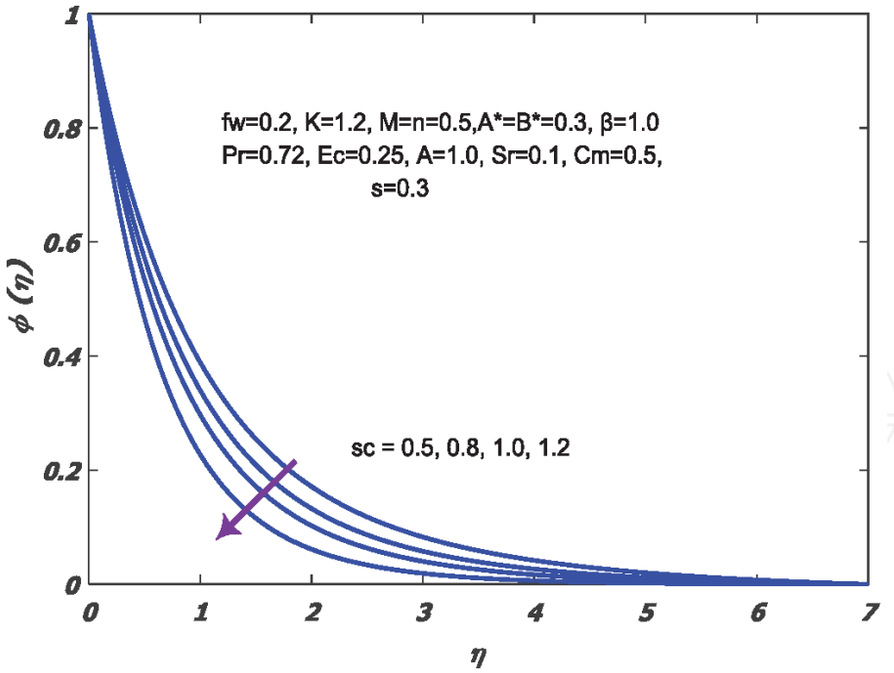

Figure 16.
Sc effects on ϕ profile.

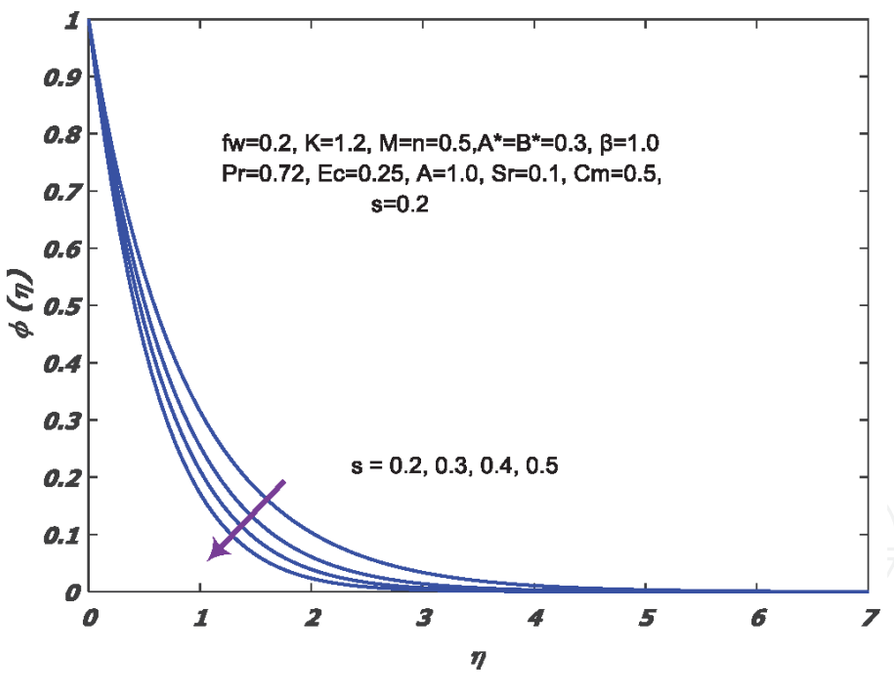

Figure 17.
s effects on ϕ profile.

2. Velocity of flow downs for growing of M, f_w.

3. For also positive value of A^* and increasing value of Ec temperature grows up

4. Mass field and corresponding boundary layers thickness downs by increasing the 'Sc'.

5. An increasing in 'Sr' causes a increase in the concentration and temperature through the boundary layer.

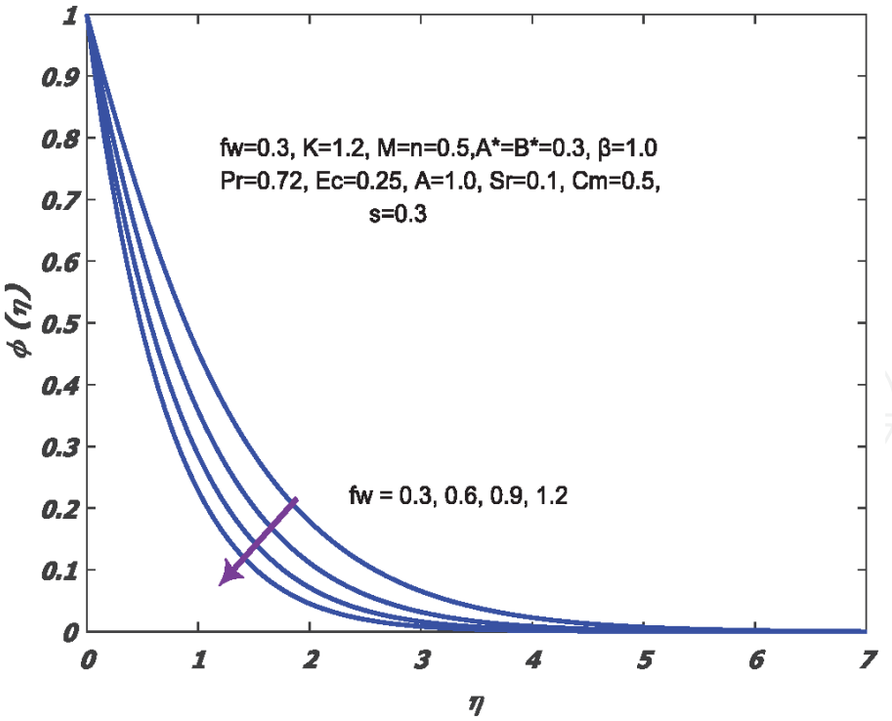

Figure 18.
f_w effects on ϕ profile.

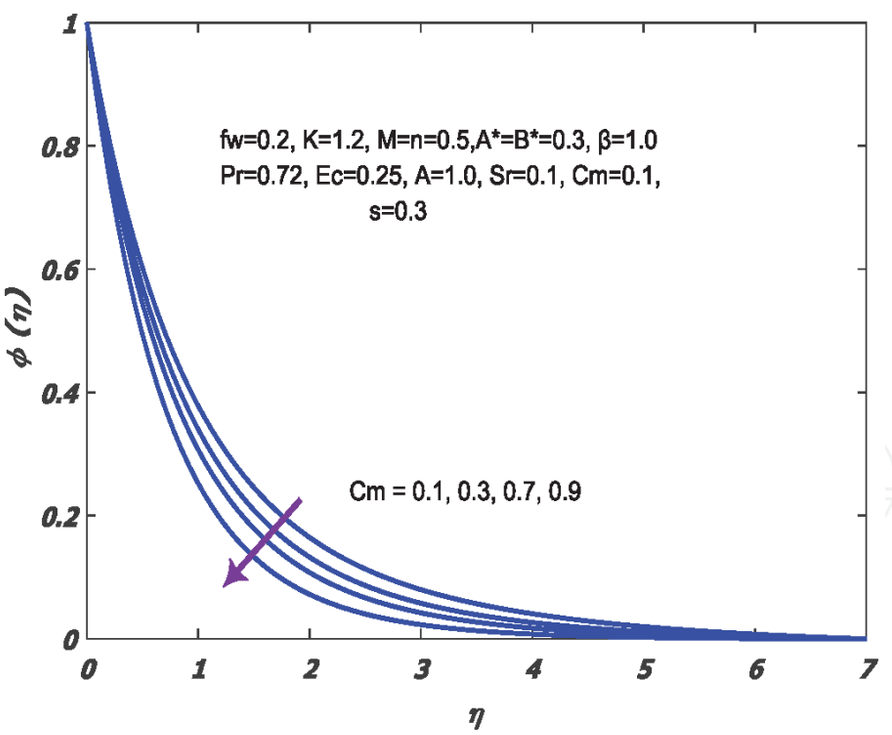

Figure 19.
Cm effects on ϕ profile.

K	A	Sc	C_m	f_w	$c_{fx}\,\mathrm{Re}_x^{1/2}$	$Nu_x(\mathrm{R}_{ex})^{-1/2}$	$M_x\,\mathrm{Re}_x$	$Sh_x/(\mathrm{R}_{ex})^{-1/2}$
0					0.3455454	1.658233	0.164237	0.7418682
0.5					0.4135856	1.668674	0.193939	0.7471964
1.0					0.482298	1.678695	0.2210438	0.7525225

K	A	Sc	C_m	f_w	$c_{fx}\,\mathrm{Re}_x^{1/2}$	$Nu_x(\mathrm{R}_{ex})^{-1/2}$	$M_x\,\mathrm{Re}_x$	$Sh_x/(\mathrm{R}_{ex})^{-1/2}$
1.5					0.5488359	1.678766	0.2460082	0.7575476
2.0					0.6130726	1.688377	0.2691283	0.7622267
0.5	0.5				0.4189335	1.668688	0.1939364	0.9283288
	1.0				0.41838978	1.688139	0.193138	0.9291135
	1.5				0.4178619	1.7081801	0.192349	0.9298976
	2.0				0.4173480	1.738553	0.191564	0.9306813
	0.5	0.5			0.4135858	1.668739	0.162426	0.7471966
		1.0			0.4319673	1.668286	0.169963	1.148792
		1.5			0.4431084	1.668264	0.174907	1.488861
		2.0			0.4507155	1.6687357	0.1785145	1.800042
		0.5	0.0		0.4014076	1.6683189	0.157579	0.1215778
			0.5		0.4135857	1.668763	0.162424	0.7471969
			1.0		0.4216537	1.6685654	0.1657039	1.148795
			1.5		0.4274917	1.668875	0.1681314	1.488867
			2.0	1.0	0.431996	1.748467	0.170059	1.800044
			0.5	0.5	0.420988	1.288242	0.212292	0.799846
				0.0	0.4189334	1.998349	0.193938	0.842233
				−0.5	0.4147433	1.808545	0.174625	0.885127
				−1.0	0.3915482	1.69878	0.1535629	0.9283398

Table 2.
Behavior of skin friction, Nusselt number, couple stress, and Sherwood number.

Nomenclature of parameters and short terms

f	Body force
l	Body couple
V	translational vector
Ω	micro-rotation vector
K	Thermal conductivity
p	Pressure
$\alpha_0, \beta_0, \gamma_0, \chi, K$	Material constants
c_s	Concentration susceptibility
M	Magnetic parameter
j	Micro-inertia
μ	dynamic viscosity
φ	dissipation function
τ	Ratio parameter
C	Concentration of fluid.
T	Temperature of the fluid
V	translational vector
Ω	micro-rotation vector
T_∞	Infinite temperature

A	Usual constant
A	Constant
a	first order slip flow parameter
T_{w}	Temperature of the plate
c_p	Specific heat
ρ	Fluid density
D_m	coefficient of mass diffusivity
α	Thermal diffusivity
Du	Dufour number,
β	Second order slip flow parameter
MPF	Micropolar fluid
$q'r'$	Non-uniform heat source
A^*, B^*	Coefficients of space and temperature
D	Mass diffusivity
K_T	Thermal diffusion ratio
D_m	Coefficient of mass diffusivity
T_m	Mean fluid temperature.
N	Constant
α^*	Slip coefficient
w	Micro rotation component
h	Heat transfer coefficient
Pr	Prandtl number
G	Micro rotation parameter
Ec,	Eckert number
σ	Reaction rate parameter
β_o	Strength of magnetic field.
Sc	Schmidt number
λ^A	Activation energy parameter
Bi_θ	Thermal Biot number
α	slip parameter
γ_1	Thermal concentration parameter.
Sr	Soret number
f_w	Suction or injection parameter
Sh_x	Sherwood number
ν	Kinematic viscosity
c_f	Skin-friction coefficient
R_{ex}	Local Reynold number
N_{ux}	Nusselt number
m_w	couple-stress
δ	Newtonian heating parameter
MHD	Magnetohydrodynamic

Author details

Assad Ayub[1], Hafiz A. Wahab[1], Zulqurnain Sabir[1] and Adnène Arbi[2,3]*

1 Department of Mathematics and Statistics, Hazara University, Manshera, Pakistan

2 Laboratory of Engineering Mathematics (LR01ES13), Tunisia Polytechnic School, University of Carthage, Tunisia

3 Department of Advanced Sciences and Technologies at National School of Advanced Sciences and Technologies of Borj Cedria, University of Carthage, Tunisia

*Address all correspondence to: adnen.arbi@gmail.com

References

[1] Herdrich, G., Auweter-Kurtz, M., Fertig, M., Nawaz, A., & Petkow, D. (2006). MHD flow control for plasma technology applications. *Vacuum*, *80* (11-12), 1167-1173.

[2] Smolentsev, S., Badia, S., Bhattacharyay, R., Bühler, L., Chen, L., Huang, Q., ... & Mistrangelo, C. (2015). An approach to verification and validation of MHD codes for fusion applications. *Fusion Engineering and Design*, *100*, 65-72.

[3] Sabir, Z., Ayub, A., Guirao, J. L., Bhatti, S., & Shah, S. Z. H. (2020). The Effects of Activation Energy and Thermophoretic Diffusion of Nanoparticles on Steady Micropolar Fluid along with Brownian Motion. *Advances in Materials Science and Engineering*, *2020*.

[4] Andersson, H. I. (1992). MHD flow of a viscoelastic fluid past a stretching surface. *Acta Mechanica*, *95*(1-4), 227-230.

[5] Raptis, A., Perdikis, C., & Takhar, H. S. (2004). Effect of thermal radiation on MHD flow. *Applied Mathematics and computation*, *153*(3), 645-649.

[6] Khan, M., Hussain, M., & Azam, M. (2016). Magnetohydrodynamic flow of Carreau fluid over a convectively heated surface in the presence of non-linear radiation. *Journal of magnetism and magnetic materials*, *412*, 63-68.

[7] Abergel, F., & Temam, R. (1990). On some control problems in fluid mechanics. *Theoretical and Computational Fluid Dynamics*, *1*(6), 303-325.

[8] Agrawal, P., Dadheech, P. K., Jat, R. N., Bohra, M., Nisar, K. S., & Khan, I. (2020). Lie similarity analysis of MHD flow past a stretching surface embedded in porous medium along with imposed heat source/sink and variable viscosity. *Journal of Materials Research and Technology*, *9*(5), 10045-10053.

[9] Aliakbar, V., Alizadeh-Pahlavan, A., & Sadeghy, K. (2009). The influence of thermal radiation on MHD flow of Maxwellian fluids above stretching sheets. *Communications in Nonlinear Science and Numerical Simulation*, *14*(3), 779-794.

[10] Khan, M. I., Hayat, T., Khan, M. I., & Alsaedi, A. (2018). Activation energy impact in nonlinear radiative stagnation point flow of Cross nanofluid. *International Communications in Heat and Mass Transfer*, *91*, 216-224.

[11] Mahanthesh, B., Gireesha, B. J., Gorla, R. R., Abbasi, F. M., & Shehzad, S. A. (2016). Numerical solutions for magnetohydrodynamic flow of nanofluid over a bidirectional non-linear stretching surface with prescribed surface heat flux boundary. *Journal of Magnetism and Magnetic Materials*, *417*, 189-196.

[12] Babu, M. J., & Sandeep, N. (2016). Three-dimensional MHD slip flow of nanofluids over a slendering stretching sheet with thermophoresis and Brownian motion effects. *Advanced Powder Technology*, *27*(5), 2039-2050.

[13] Nadeem, S., Haq, R. U., & Akbar, N. S. (2013). MHD three-dimensional boundary layer flow of Casson nanofluid past a linearly stretching sheet with convective boundary condition. *IEEE Transactions on Nanotechnology*, *13* (1), 109-115.

[14] T. Armin, M.A. Turk, N.D. Sylvester, Application of microcontinuum fluid mechanics, Int. J. Engng. Sci. 12 (1974) 273–279.

[15] V.M. Soundalgekar, H.S. Takhar, Flow of a micropolar fluid on a

continuous moving plate, Int. J. Engng. Sci. 21 (1983) 961– 965.

[16] F.M. Hady, Short communication on the solution of heat transfer to micropolar fluid from a non-isothermal stretching sheet with injection, Int J. Num. Meth. Heat Fluid Flow 6 (1996) 99–104.

[17] A. Ishak, R. Nazar, I. Pop, Heat transfer over a stretchingsurface with variable surface heat flux in micropolar fluids, Phys. Lett. A 372 (2008) 559–561.

[18] I.A. Hassanien, R.S.R. Gorla, Heat transfer to a micropolar fluid from a non-isothermal stretching sheet with suction and blowing, Acta Mech. 84 (1990) 191–199.

[19] T. Hayat, Z. Abbas, T. Javed, Mixed convection flow of a micropolar fluid over a non-linear stretching sheet, Phys. Lett. A372 (2008) 637–647.

[20] T. Hayat, T. Javed, Z. Abbas, MHD flow of a micropolar fluid near a stagnation-point towards a non-linear stretching surface, Nonlinear Anal.: Real World Appl. 10 (2009) 1514–1526.

[21] M. Sajid, N. Ali, T. Hayat, On exact solutions for thin film flows of a micropolar fluid, Commun. Nonlinear Sci. Num. Simul. 14 (2009) 451–461.

[22] M. Sajid, Z. Abbas, T. Hayat, Homotopy analysis for boundary layer flow of a micropolar fluid through a porous channel, Appl. Math. Model. 33 (2009) 4120–4125.

[23] Alsaedi, A., Awais, M., & Hayat, T. (2012). Effects of heat generation/ absorption on stagnation point flow of nanofluid over a surface with convective boundary conditions. *Communications in Nonlinear Science and Numerical Simulation*, *17*(11), 4210-4223.

[24] Mabood, F., Ibrahim, S. M., Rashidi, M. M., Shadloo, M. S., & Lorenzini, G. (2016). Non-uniform heat source/sink and Soret effects on MHD non-Darcian convective flow past a stretching sheet in a micropolar fluid with radiation. *International Journal of Heat and Mass Transfer*, *93*, 674-682.

[25] Reddy, M. G., & Reddy, N. B. (2011). Mass transfer and heat generation effects on MHD free convection flow past an inclined vertical surface in a porous medium.

[26] R. Ravindran, M. Ganapathirao, I. Pop, Effects of chemical reaction and heat generation/absorption on unsteady mixed convection MHD flow overa vertical cone with non-uniform slot mass transfer, Int.J.Heat & Mass Transfer 73 (2014) 743-751.

[27] Ghadikolaei, S. S., Hosseinzadeh, K., Ganji, D. D., & Jafari, B. (2018). Nonlinear thermal radiation effect on magneto Casson nanofluid flow with Joule heating effect over an inclined porous stretching sheet. *Case Studies in Thermal Engineering*, *12*, 176-187.

[28] N, Sandeep, C, Sulochana, Dual solutions for unsteady mixed convection flow of MHD micropolar fluid over a stretching /shrinking sheet with nonuniform heat source/sink, JESTECH. 18 (2015) 738-745.

[29] Hayat, T., Khan, M. I., Tamoor, M., Waqas, M., & Alsaedi, A. (2017). Numerical simulation of heat transfer in MHD stagnation point flow of Cross fluid model towards a stretched surface. *Results in physics*, *7*, 1824-1827.

[30] Damseh, R. A., Al-Odat, M. Q., Chamkha, A. J., & Shannak, B. A. (2009). Combined effect of heat generation or absorption and first-order chemical reaction on micropolar fluid flows over a uniformly stretched permeable surface. *International Journal of Thermal Sciences*, *48*(8), 1658-1663.

[31] Das, K. (2011). Effect of chemical reaction and thermal radiation on heat

and mass transfer flow of MHD micropolar fluid in a rotating frame of reference. *International journal of heat and mass transfer*, *54*(15-16), 3505-3513.

[32] Magyari, E., & Chamkha, A. J. (2010). Combined effect of heat generation or absorption and first-order chemical reaction on micropolar fluid flows over a uniformly stretched permeable surface: the full analytical solution. *International Journal of Thermal Sciences*, *49*(9), 1821-1828.

[33] Yokuş, A., & Gülbahar, S. (2019). Numerical solutions with linearization techniques of the fractional Harry Dym equation. *Applied Mathematics and Nonlinear Sciences*, *4*(1), 35-42.

[34] Sajid T., Sabir Z., Tanveer S., Arbi A., Altamirano GC. (2020). Upshot of radiative rotating Prandtl fluid flow over a slippery surface embedded with variable species diffusivity and multiple convective boundary conditions. *Heat Transfer*. 2020;1–21. https://doi.org/10.1002/htj.22010

[35] Dewasurendra, M., & Vajravelu, K. (2018). On the method of inverse mapping for solutions of coupled systems of nonlinear differential equations arising in nanofluid flow, heat and mass transfer. *Applied Mathematics and Nonlinear Sciences*, *3*(1), 1-14.

[36] Dusunceli, F. (2019). New exact solutions for generalized (3+ 1) shallow water-like (SWL) equation. *Applied Mathematics and Nonlinear Sciences*, *4* (2), 365-370.

[37] Yokus, A., Durur, H., & Ahmad, H. (2020). Hyperbolic type solutions for the couple Boiti-Leon-Pempinelli system. *Facta Universitatis, Series: Mathematics and Informatics*, *35*(2), 523-531.

[38] Ali, M., Shahzad, M., Sultan, F., Khan, W. A., & Shah, S. Z. H. (2020). Characteristic of heat transfer in flow of Cross nanofluid during melting process. *Applied Nanoscience*, 1-10.

[39] Pérez-García, V. M., Fitzpatrick, S., Pérez-Romasanta, L. A., Pesic, M., Schucht, P., Arana, E., & Sánchez-Gómez, P. (2016). Applied mathematics and nonlinear sciences in the war on cancer. *Applied Mathematics and Nonlinear Sciences*, *1*(2), 423-436.

[40] Shah, S. Z., Wahab, H. A., Ayub, A., Sabir, Z., Haider, A., & Shah, S. L. Higher order chemical process with heat transport of magnetized cross nanofluid over wedge geometry. Heat Transfer.